Materials Advances

ROYAL SOCIETY OF CHEMISTRY

PAPER

View Article Online
View Journal | View Issue

Cite this: *Mater. Adv.*, 2022, 3, 7960

Magnetically recoverable Cu_2O–Fe_3O_4@TNT catalytic system for click chemistry in water: multi-component synthesis of 1,2,3-triazoles at room temperature†

Venkata Ramana Kumar Velpula,[ab] Thirupathaiah Ketike,[a] Anusha Rajajagdeesan,[c] Manisha Atul Bora,[d] Saidulu Ganji,*[e] David Raju Burri[ab] and Krishna Mohan Surapaneni[c]

Received 22nd April 2022,
Accepted 7th August 2022

DOI: 10.1039/d2ma00451h

rsc.li/materials-advances

The catalytic performance of a Cu_2O–Fe_3O_4@TNT nanocatalyst derived from Fe(III) acetylacetonate, Cu(II) acetylacetonate and hydrogen titanate nanotubes (HTNTs) has been investigated for the first time for the click reaction in a water medium at room temperature. The nanocatalyst was characterized by performing XRD, HR-TEM, XPS, UV-DRS, H_2-TPR, N_2 adsorption-desorption, and ICP-OES analyses. The catalyst showed superior catalytic activity for the multicomponent synthesis of 1,2,3-triazoles in an aqueous medium. The nanocatalyst can be reused and recovered by using an external magnet.

Introduction

Click chemistry shortens the procedure for synthesizing 1,4-disubstituted 1,2,3-triazoles, providing quicker detection and optimization.[1] Various triazoles have found clinical applications, such as in anti-bacterial agents[2] and those displaying anti-HIV activity[1a,3] as well as for β3-adrenergic receptor agonism.[4] Also, triazoles are incorporated in dyes, herbicides, and fungicides.[5] Cu-Catalyzed construction of triazole derivatives has been carried out by using a convenient scheme involving N_3^--alkyne cycloaddition. Many homogeneous and heterogeneous catalysts have been developed for this (CuAAC) reaction. Included among the several heterogeneous catalytic systems that have been developed recently are Cu[1]-zeolite,[6] a complex of NHC and Cu(I),[7,8] Cu nanoparticles,[9,10] a Cu_2O catalyst,[11,12] and magnetically separable catalysts.[13–15]

The ability to remove as much Cu as possible from a solution is a priority, particularly for biological applications.[16] For pharmaceuticals, the permeability limits for metal content are <10 ppm.[17] In this context, nano-catalysis has been developed as a modest and sustainable alternative to traditional catalysis because of the large surface-to-volume ratios of the nanoparticles, which increase their activity and selectivity, preserving the inherent characteristics of a heterogeneous catalyst.[18]

Inorganic supports having large surface areas can be used to capture metal nanoparticles and form especially active and recyclable catalysts as a result of the relatively high stability and dispersion of the particles. Various strategies involving centrifugation or filtration, often used for isolating catalysts in general, are unsustainable, noneconomic, outdated and particularly unsuitable for isolating nanosized catalysts. These strategies can be avoided when using magnetic nanoparticles (MNPs), which can be isolated by using an external magnet in a simple and efficient method to remove such nanocatalysts from reaction mixtures, and such retrieved MNPs have been shown to be ideal catalysts or supports. This alternative strategy has received excellent reviews.[19]

Hydrogen titanate nanotubes (HTNTs) have been intensively studied, attracting much attention in the past decade due to their unique textural and physicochemical properties, including versatile applications, particularly in catalysis and photocatalysis. Titanate NTs that are synthesized from TiO_2 nanoparticles (particle size $<$ 25 nm) using the hydrothermal method display high specific surface areas ($\approx$200–400 $m^2\ g^{-1}$), and are widely used because of their high amenability to being modified as desired. While the preparation of titanate NTs from TiO_2 nanoparticles is well established, procedures for

[a] *Indian Institute of Chemical Technology, Department of Catalysis & Fine Chemicals, Tarnaka, Hyderabad-500007, India*
[b] *Academy of Scientific and Innovative Research (AcSIR), Sector 19, Kamla Nehru Nagar, Ghaziabad, Uttar Pradesh 201002, India*
[c] *Department of Biochemistry, Panimalar Medical College Hospital & Research Institute, Varadharajapuram, Poonamallee, Chennai – 600 123, Tamil Nadu, India*
[d] *B.J.S.'S Arts, Science & Commerce College, Wagholi, Pune, Maharashtra, 412207, India*
[e] *Department of Chemistry, J B Institute of Engineering and Technology (UGC Autonomous), Hyderabad, 500075, India. E-mail: saiduluganji@gmail.com*

† Electronic supplementary information (ESI) available. See DOI: https://doi.org/10.1039/d2ma00451h

preparing them from commercial TiO_2 powder are limited. The most important and attractive material for magnetic applications is nanostructured magnetite (Fe_3O_4), due to its biocompatibility, high magnetic susceptibility, chemical stability, innocuousness, high saturation magnetization, and inexpensiveness.[22–25]

As part of our ongoing interest in developing metal nanocatalysts for organic transformations in aqueous media,[26–28] in our current work we developed a design and synthesis of the magnetically active nanocatalyst Cu_2O–Fe_3O_4 supported on hydrogenated titanium NTs (Cu_2O–Fe_3O_4@TNT) and effectively used it to catalyze the synthesis of 1,4-disubstituted 1,2,3-triazoles at room temperature in an eco-friendly medium involving the use of water as the solvent. The details of the preparation, characterization, and applications of the catalyst are described.

Experimental

All chemicals were received from commercial sources and used as received.

Preparation of catalysts

HTNT synthesis. Hydrogen titanate NTs were prepared *via* a hydrothermal method. Typically, 3.5 g of TiO_2 were dispersed in an aqueous solution of NaOH (10 M, 200 ml), and the resulting mixture was sonicated for 30 minutes and then transferred into a 300 ml Teflon-lined stainless-steel autoclave and kept there at 130 °C for 20 h (for NTs) and into a Teflon-lined autoclave at 180 °C per 20 h (for nanorods). The white precipitate in the autoclave was washed repeatedly with deionized water followed by dispersing the residues in 0.1 N HCl (100 ml) under stirring for 24 h.

Synthesis of Cu_2O and Fe_3O_4 nanoparticles. A mass of 3.5 g of iron(III) acetylacetonate and 1.4 g of Cu(III) acetylacetonate were together dissolved in 100 ml of oleylamine and then subjected to hydrothermal treatment in a 250 ml autoclave under an N_2 atmosphere at 300 °C for 12 h. The resultant solution was poured into 500 ml of ethanol and the formed precipitate was collected and subjected to centrifugation after being redispersed in 100 ml of petroleum ether. Again the precipitate was dispersed in 100 ml of ethanol and100 ml of petroleum ether solution collected the sediment, and this process was repeated five times. The final obtained nanoparticles were allowed to dry at RT for one day.

Preparation of Cu_2O–Fe_3O_4@TNT catalyst. A mass of 0.8 g of HTNT was dispersed into 50 ml of petroleum ether and a mass of 0.2 g of Cu_2O–Fe_3O_4 nanoparticles was dispersed into a separate 50 ml sample of petroleum ether, and each resulting dispersion was subjected to sonication for 30 minutes. The resulting latter solution was slowly added to the former under sonication, which was then continued for another 15 minutes. Catalyst was collected from the resultant mixture by using an external magnet and dried at 80 °C for 24 h. The amounts of Cu and Fe present in the collected catalyst were determined using ICP-OES.

Results and discussion

XRD studies

The XRD pattern of commercially purchased TiO_2 powder shown in Fig. 1 indicated that it was in the anatase form in accordance with the diffraction peak positions at 2θ = 25.4, 37.9, 48.0, 54.0, 55.1, 62.7, 68.8, 70.4 and 75.1° and the corresponding (101), (004), (200), (105), (211), (204), (116), (200) and (215) crystal planes (JCPDS: 01-07-2486C). The XRD pattern of $H_2Ti_3O_7$ was poorly resolved, confirming the transformation of highly crystalline anatase TiO_2 into a nanoscopic material. Nevertheless, in this pattern, four diffraction peaks at 2θ = 11.2, 24.1, 28.5, and 48.5 and assigned to $H_2Ti_3O_7$ were discerned, and the low-angle peaks indicated the layered structure of HTNT. The intensities at 2θ = 35.5, 57.5, and 62.8° originated from the magnetite Fe_3O_4 nanoparticles; note, in comparison, the standard XRD data for Fe_3O_4 (JCPDS No. 19-0629). The diffraction peaks at 29.6, 35.7, 43.52, and 62.84° derived from Cu_2O (JCPDS No. 05-0667). The presence of Cu_2O and Fe_3O_4 was confirmed using other analytical techniques, namely XPS, UV-DRS, and H_2-TPR.

TPR studies for Cu_2O–Fe_3O_4@HTNT

The TPR profile of Cu_2O–Fe_3O_4@HTNT (Fig. 2) showed a reduction temperature region from 160 to 220 °C, attributed to the transformation Cu_2O(I) → Cu (0). Note that the presence of Cu_2O was also confirmed from XPS data.[20] A small sharp peak was also observed at 400 °C, and corresponded to H_2 consumption responsible for the transformation of Fe_2O_3 to Fe_3O_4, (maghemite → magnetite). In addition, a broad peak from 450 to 650 °C was observed, and was attributed to the conversion of Fe_3O_4 to FeO (magnetite → wustite).[21]

XPS studies

As shown in Fig. 3(b), the high-resolution XPS data for Cu_2O–Fe_3O_4@HTNT showed two prominent peaks and one satellite peak

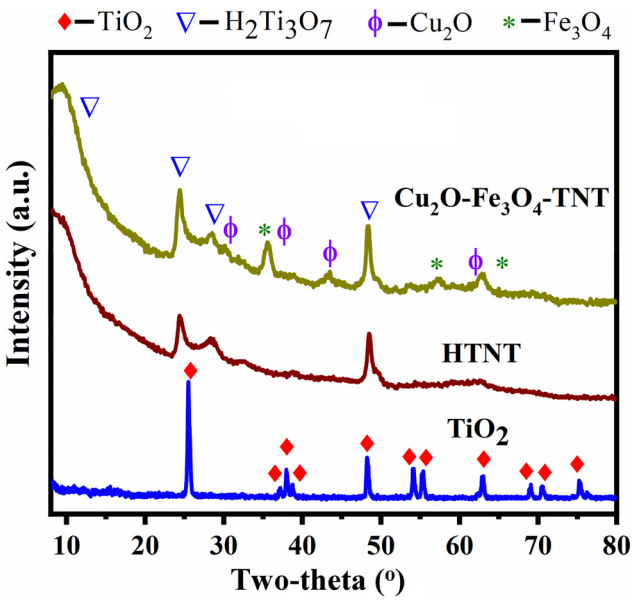

Fig. 1 XRD patterns of TiO_2, TNT, and Cu_2O–Fe_3O_4@TNT.

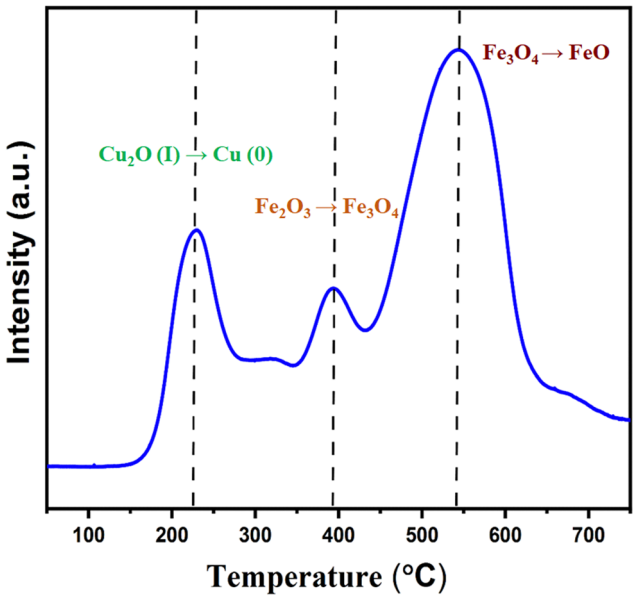

Fig. 2 H_2-TPR of Cu_2O–Fe_3O_4@TNT.

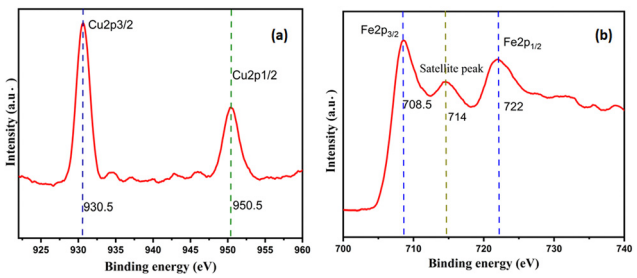

Fig. 3 XPS patterns of Cu_2O–Fe_3O_4@HTNT in the (a) Cu and (b) Fe regions.

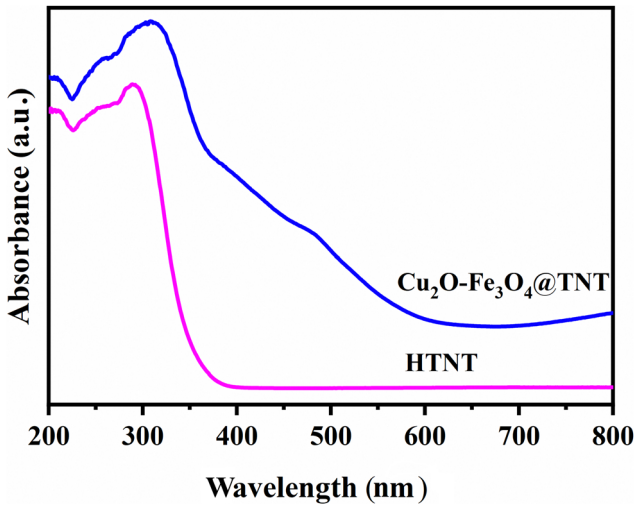

Fig. 4 UV-DRS spectrum of HTNT and Cu_2O–Fe_3O_4@TNT.

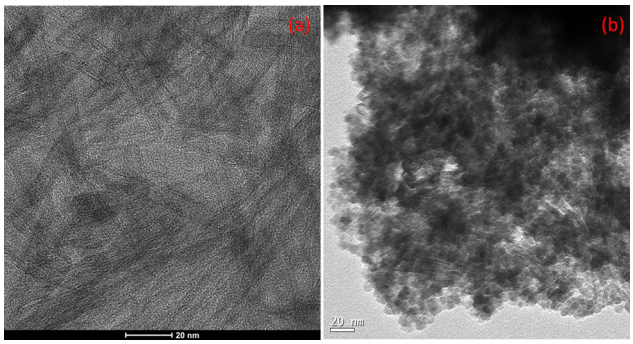

Fig. 5 TEM images of (a) HTNT and (b) the Cu_2O–Fe_3O_4@TNT catalyst.

in the Fe 2p region, specifically one peak at 722 eV and corresponding to Fe $2p_{1/2}$, the other peak at 708.5 eV and corresponding to Fe $2p_{3/2}$, and the satellite peak at 714 eV. The two spin–orbit couplings at Fe $2p_{1/2}$ and Fe $2p_{3/2}$ were attributed to Fe^{2+} and Fe^{3+}. These results for Fe_3O_4 agreed with the literature.[32] As shown in Fig. 3(a), the Cu 2p region showed two prominent peaks, at 930.5 eV and 950.5 eV and corresponding to Cu $2p_{3/2}$ and Cu $2p_{1/2}$, respectively, and indicating the presence of Cu_2O.

UV-visible studies

Optical properties of the catalysts were investigated by performing UV-Vis absorption studies. As shown in Fig. 4, the Cu_2O–Fe_3O_4@TNT catalyst showed a broad absorption with the characteristic peak of Cu_2O at a wavelength of 490 nm and the free excitation peak at 421 nm.[29–31]

TEM analysis

TEM images of our samples are shown in Fig. 5. Inspection of these images indicated that the titanate NTs produced from titanium powder retained their tubular structure with an internal diameter of 4.834 nm and interlayer distance of 0.35 nm—and that when Cu_2O and Fe_3O_4 were introduced onto the HTNTs, the surfaces of the NTs became entirely shielded with Cu_2O, Fe_3O_4 nanoparticles. Here, an average particle size of 5.5 nm was calculated from the latter TEM image.

Activity test

The newly amassed catalyst (Cu_2O–Fe_3O_4@TNT) was then tested for its ability to promote click addition through the reaction of terminal alkynes with *in situ*-generated organic azide. This one-pot procedure offered the benefit of not needing to pre-synthesize the azido partner, in contrast to the case for most nanoparticle-catalyzed click reactions. The reaction was carried out at room temperature, under air, using 50 mg of the catalyst, 7 mmol of phenyl acetylene, 7.5 mmol of NaN_3 and 5 mmol of alkyl or benzyl halide in 5 ml of water. After completion of the reaction, ethyl acetate solvent was used to dissolve the product formed and the catalyst was recovered using an external magnet; the products were collected by concentrating the residual solution.

The results of various test reactions are listed in Table 1. The reaction neither occurred without catalyst nor with HTNT.

Table 1 Reaction optimization conditions

Entry	Catalyst	Amount of catalyst (mg)	Time (h)	Yield (%)
1	HTNT	20	12	0
2	No catalyst	—	12	0
3	Cu_2O–Fe_3O_4@TNT	20	4	54
4	Cu_2O–Fe_3O_4@TNT	30	4	82
5	Cu_2O–Fe_3O_4@TNT	50	4	98
6	Cu_2O–Fe_3O_4@TNT	70	4	86
7[a]	Cu_2O–Fe_3O_4@TNT	50	4	93
8[b]	Cu_2O–Fe_3O_4@TNT	50	4	98
9[c]	Cu_2O–Fe_3O_4@TNT	50	4	67

Benzyl bromide (5 mmol), NaN_3 (7.5 mmol), alkyne (7 mmol), and Cu_2O–Fe_3O_4@TNT (50 mg), solvent = water (5 ml), stirred at RT for 4 h [a] Reaction at 60 °C. [b] Reaction at 100 °C. [c] Neat at RT.

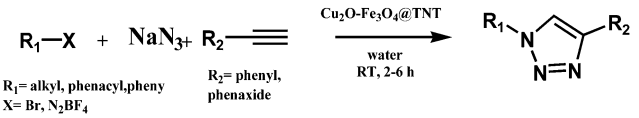

Scheme 1 Click reaction over Cu_2O–Fe_3O_4@TNT catalyst.

The reaction progressed with Cu_2O–Fe_3O_4@TNT catalyst, indicating the need of having active metal to perform the reaction (Scheme 1).

The catalytic system proved efficient on a variety of substrates (Table 2) and was active on various terminal alkynes such as phenyl acetylene derivatives. The structures of all of the isolated compounds (yields ranging from 95 to 99%) were confirmed from ^{1}H-NMR data.

The most important advantage of carrying out the CuAAC reaction in an aqueous solvent was the easy isolation of analytically clean products, that is by removing the catalyst with an external magnet. The solid resulting from the reaction was then dissolved in an ethyl acetate solution; concentrating the residual solution gave clean products without the need for any tedious column isolation. The magnetically separated

Table 2 Scope of the reaction

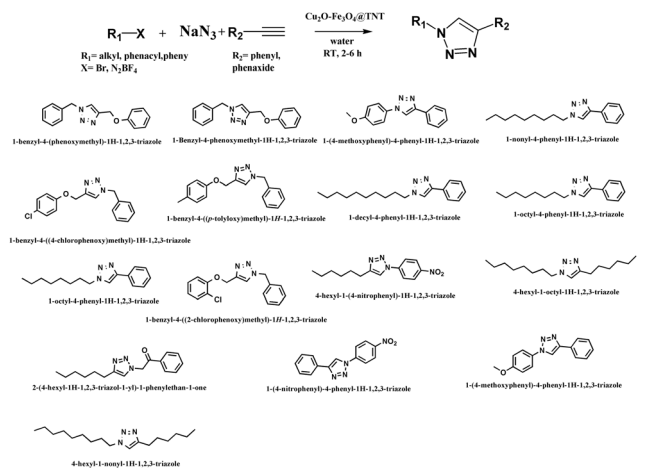

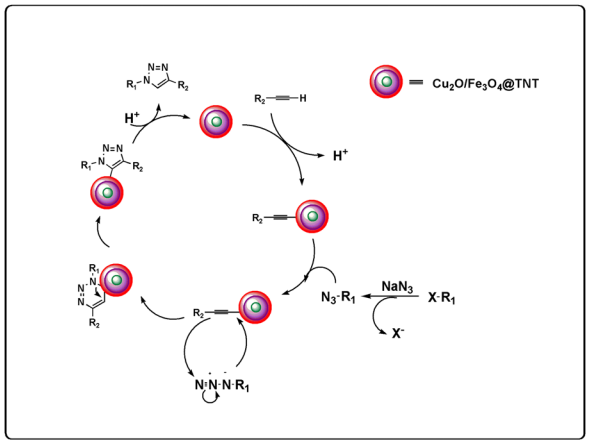

Fig. 6 Proposed mechanism.

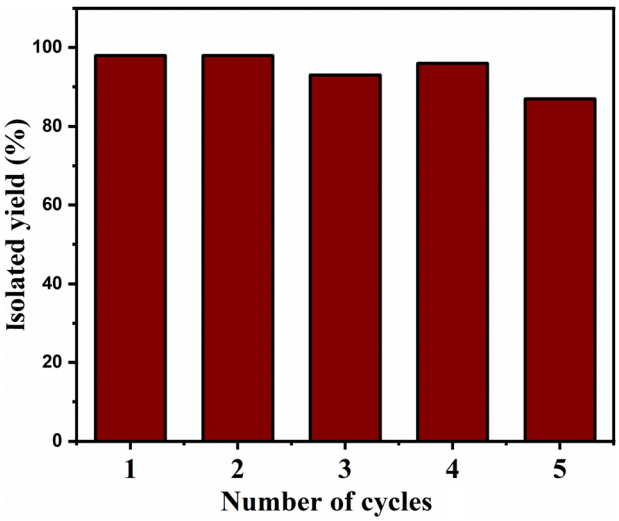

Fig. 7 Recyclability of the Cu_2O–Fe_3O_4@TNT catalyst.

catalyst was washed with ethyl acetate twice and dried at 100 °C in a hot air oven for 12 h and used for the next run.

A mechanism has been proposed based on our experimental results and previous reports,[33] and the details of this mechanism are shown in Fig. 6.

Recyclability test

The catalyst was re-used four times and still led to a decent product yield, as depicted in Fig. 7. At the end of each cycle, the catalyst was collected by using an external magnet, washed with ethyl acetate thrice, and dried in a hot air oven at 100 °C for 12 h to be used for the next cycle.

Conclusions

A novel magnetically recoverable Cu_2O–Fe_3O_4@TNT catalyst was synthesized. The performance of the catalyst towards the click reaction for the synthesis of 1,4-disubstituted 1,2,3-triazoles *via in situ*-liberated organic azide with alkynes was

established. The very high activity of catalyst was concluded to be due to the particles of Cu in the Cu^{1+} state. The catalyst can be used for the synthesis of a wide variety of substrates.

Conflicts of interest

There are no conflicts to declare.

Acknowledgements

V. R. K. Velpula and T. Ketike are thankful to Council of Scientific and Industrial Research (CSIR) and UGC, New Delhi, India, for research fellowships.

Notes and references

1 (*a*) P. W. Baures, *Org. Lett.*, 1999, **1**, 249; (*b*) A. K. Jordão, V. F. Ferreira, T. M. L. Souza, G. G. D. S. Faria, V. Machado, J. L. Abrantes, M. C. B. V. de Souza and A. C. Cunha, *Bioorg. Med. Chem.*, 2011, **19**, 1860; (*c*) L. S. Kallander, Q. Lu, W. Chen, T. Tomaszek, G. Yang, D. Tew, T. D. Meek, G. A. Hofmann, C. K. S. Pritchard, W. W. Smith, C. A. Janson, M. D. Ryan, G. F. Zhang, K. O. Johanson, R. B. Kirkpatrick, T. F. Ho, P. W. Fisher, M. R. Mattern, R. K. Johnson, M. J. Hansbury, J. D. Winkler, K. W. Ward, D. F. Veber and S. K. Thompson, *J. Med. Chem.*, 2005, **48**, 5644; (*d*) S. G. Agalave, S. R. Maujan and D. V. S. Pore, *Chem. – Asian J.*, 2011, **6**, 2696; (*e*) A. Lauria, R. Delisi, F. Mingoia, A. Terenzi, A. Martorana, G. Barone and A. M. Almerico, *Eur. J. Org. Chem.*, 2014, 3289–3306; (*f*) R. Aggarwal and G. Sumran, *Eur. J. Med. Chem.*, 2020, **205**, 112652; (*g*) P. Thirumurugan, D. Matosiuk and K. Jozwiak, *Chem. Rev.*, 2013, **113**, 4905–4979; (*h*) D. Dheer, V. Singh and R. Shankar, *Bioorg. Chem.*, 2017, **71**, 30–54; (*i*) G. Mohammad and J. Neda, *ACS Sustainable Chem. Eng.*, 2014, **2**(12), 2658–2665; (*j*) G. Mohammad, O. Erfan and M. S. Jose, *ChemistrySelect*, 2019, **4**, 3151–3160.

2 M. J. Genin, D. K. Hutchinson, D. A. Allwine, J. B. Hester, D. E. Emmert, S. A. Garmon, C. W. Ford, G. E. Zurenko, J. C. Hamel, R. D. Schaadt, D. Stapert, B. H. Yagi, J. M. Friis, E. M. Shobe and W. J. Adams, *J. Med. Chem.*, 2000, **43**, 953.

3 R. Alvarez, S. Velazquez, A. San-Felix, S. Aquaro, E. De Clercq, C. F. Perno, A. Karlsson, J. Balzarini and M. J. Camarasa, *J. Med. Chem.*, 1994, **37**, 4185.

4 L. L. Brockunier, E. R. Parmee, H. O. Ok, M. R. Candelore, M. A. Cascieri, L. F. Colwell, L. Deng, W. P. Feeney, M. J. Forrest, G. J. Hom, D. E. MacIntyre, L. Tota, M. J. Wyvratt, M. H. Fisher and A. E. Weber, *Bioorg. Med. Chem. Lett.*, 2000, **10**, 2111.

5 H. Wamhoff, *Comprehensive Heterocyclic Chemistry*, Pergamon, Oxford, 1984, vol. 5, p. 669.

6 V. Beneteau, A. Olmos, T. Boningari, J. Sommer and P. Pale, *Tetrahedron Lett.*, 2010, **51**, 3673–3677.

7 M. A. Topchiy, A. A. Ageshina, P. S. Gribanov, S. M. Masoud, T. R. Akmalov, S. E. Nefedov, S. N. Osipov, T. R. Akmalov and A. F. Asachenko, *Eur. J. Org. Chem.*, 2019, 1016–1020.

8 A. Mishra, P. Rai, M. Srivastava, B. P. Tripathi, S. Yadav, J. Singh and J. Singh, *Catal. Lett.*, 2017, **147**, 2600–2611.

9 M. Nasrollahzadeh, B. Jaleh, P. Fakhri, A. Zahraei and E. Ghadery, *RSC Adv.*, 2015, **5**, 2785.

10 W. B. Yu, L. X. Jiang, C. Shen, W. M. Xu and P. F. Zhang, *Catal. Commun.*, 2016, **79**, 11–16.

11 Y. H. Tsai, K. Chanda, Y. T. Chu, C. Y. Chiu and M. H. Huang, *Nanoscale*, 2014, **6**, 8704–8709.

12 R. P. R. Bhoomireddy, L. G. B. Narla and V. G. R. Peddiahgari, *Appl. Organomet. Chem.*, 2019, **33**, e4752.

13 A. Salamatmanesh, M. K. Miraki, E. Yazdani and A. Heydari, *Catal. Lett.*, 2018, **148**, 3257–3268.

14 Y. Jain, M. Kumari, R. P. Singh, D. Kumar and R. Gupta, *Catal. Lett.*, 2020, **150**, 1142–1154.

15 R. Bonyasi, M. Gholinejad, F. Saadati and C. Najera, *New J. Chem.*, 2018, **42**, 3078–3086.

16 (*a*) R. Wang, X. T. Wang, L. Wu, M. A. Mateescu and J. Toxicol, *Environ. Health Part A*, 1999, **57**, 507; (*b*) M. K. Rauf, I. Din, A. Badshah, M. Gielen, M. Ebihara, D. de Vos and S. Ahmed, *J. Inorg. Biochem.*, 2009, **103**, 1135; (*c*) M. L. Teyssot, A. S. Jarrousse, A. Chevry, A. De Haze, C. Beaudoin, M. Manin, S. P. Nolan, S. Díez-González, L. Morel and A. Gautier, *Chem. – Eur. J.*, 2009, **15**, 314.

17 M. Crevoisier, E. L. Barle, A. Flueckiger, D. G. Dolan, M. Ovais and A. Walsh, *Pharm. Dev. Technol.*, 2016, **1**, 52–56.

18 (*a*) *Nanoparticles and Catalysis*, ed. D. Astruc, Wiley-VCH, Weinheim, Germany, 2008; (*b*) *Selective Nanocatalysts and Nanoscience: Concepts for Heterogeneous and Homogeneous Catalysis*, ed. A. Zecchina, S. Bordiga and E. Groppo, Wiley-VCH, Weinheim, Germany, 2011; (*c*) *Nanomaterials in Catalysis*, ed. P. Serp and K. Philippot, Wiley-VCH, Weinheim, Germany, 2013; (*d*) Y. Xia, H. Yang and C. T. Campbell, *Acc. Chem. Res.*, 2013, **46**, 1671–1910.

19 (*a*) A.-H. Lu, E. L. Salabas and F. Schüth, *Angew. Chem., Int. Ed.*, 2007, **46**, 1222; (*b*) S. Shylesh, V. Schünemann and W. R. Thiel, *Angew. Chem., Int. Ed.*, 2010, **49**, 3428; (*c*) Y. Zhu, L. P. Stubbs, F. Ho, R. Liu, C. P. Ship, J. A. Maguire and N. S. Hosmane, *ChemCatChem*, 2010, **2**, 365; (*d*) V. Polshettiwar, R. Luque, A. Fihri, H. Zhu, M. Bouhrara and J. M. Basset, *Chem. Rev.*, 2011, **111**, 3036; (*e*) L. M. Rossi, M. A. S. Garcia and L. L. R. J. Braz. Vono, *Chem. Soc.*, 2012, **23**, 1959; (*f*) R. B. N. Baig and R. S. Varma, *Chem. Commun.*, 2013, **49**, 752; (*g*) B. Karimi, F. Mansouri and H. M. Mirzaei, *Chem. Rev.*, 2014, **114**, 6949–6985.

20 Y. Zhai, Y. Ji, G. Wang, Y. Zhu, H. Liu, Z. Zhong and F. Su, *RSC Adv.*, 2015, **5**, 73011.

21 S. S. Kim, S. M. Lee and S. C. Hong, *J. Ind. Eng. Chem.*, 2012, **2**, 860–864.

22 Y. M. Huh, Y. Jun, H. T. Song, S. Kim, J. Choi, J. H. Lee, S. Yoon, K. S. Kim, J. S. Shin, J. S. Suh and J. Cheon, *J. Am. Chem. Soc.*, 2005, **127**, 12387.

23 J. M. Perez, L. Josephson, T. O'Loughlin, D. Hogemann and R. Weissleder, *Nat. Biotechnol.*, 2002, **20**, 816.

24 S. Sun and H. Zeng, *J. Am. Chem. Soc.*, 2002, **124**, 8204.

25 Z. Xu, C. Shen, Y. Hou, H. Gao and S. Sun, *Chem. Mater.*, 2009, **21**, 1778–1780.

26 S. Ganji, S. Mutyala, C. K. P. Neeli, K. S. Rama Rao and D. R. Burri, *RSC Adv.*, 2013, **3**, 11533.
27 S. Ganji, S. S. Enumula, R. K. Marella, K. S. Rama Rao and D. R. Burri, *Catal. Sci. Technol.*, 2014, **4**, 1813.
28 S. Ganji, P. Bukya, Z. W. Liu, K. S. Rama Rao and D. R. Burri, *New J. Chem.*, 2019, **43**, 11871.
29 Y. Pan, S. Deng, L. Polavarapu, N. Gao, P. Yuan, C. H. Sow and Q. Xu, *Langmuir*, 2012, **28**, 12304–12310.
30 J. Kou, A. Saha, C. B. Stamper and R. S. Varma, *Chem. Commun.*, 2012, **48**, 5862–5864.
31 L. Liu, S. Lin, J. Hu, Y. Liang and W. Cui, *Appl. Surf. Sci.*, 2015, **330**, 94–103.
32 C. L. C. Carvalho, A. T. B. Silva, R. A. S. Luz, G. M. B. Castro, C. L. Lima, V. R. Mastelaro, R. R. D. Silva, O. N. Oliveira and W. C. Silva, *ACS Appl. Nano Mater.*, 2018, **1**(8), 4283–4293.
33 (*a*) H. B. E. Ayouchia, L. Bahsis, H. Anane, L. R. Domingo and S.-E. Stiriba, *RSC Adv.*, 2018, **8**, 7670–7678; (*b*) V. V. Rostovtsev, L. G. Green, V. V. Fokin and K. B. Sharpless, *Angew. Chem., Int. Ed.*, 2002, **41**, 2596–2599; (*c*) C. W. Tornøe, C. Christensen and M. Melda, *J. Org. Chem.*, 2002, **67**, 3057–3064.